Biochemical and Biophysical Research Communications 435 (2013) 313–318

Contents lists available at SciVerse ScienceDirect

Biochemical and Biophysical Research Communications

journal homepage: www.elsevier.com/locate/ybbrc

In vivo phosphorylation and *in vitro* autophosphorylation-inactivation of *Kluyveromyces lactis* hexokinase KlHxk1

Karina Kettner [a,*,1], E. Bartholomeus Kuettner [b,1], Albrecht Otto [c,3], Hauke Lilie [d], Ralph P. Golbik [d], Norbert Sträter [b,2], Thomas M. Kriegel [a,2]

[a] Institute of Physiological Chemistry, Carl Gustav Carus Medical Faculty, Technische Universität Dresden, Fiedlerstrasse 42, D-01307 Dresden, Germany
[b] Institute of Bioanalytical Chemistry, Center for Biotechnology and Biomedicine, Faculty of Chemistry and Mineralogy, Leipzig University, Deutscher Platz 5, D-04103 Leipzig, Germany
[c] Max Delbrück Center for Molecular Medicine, Neuroproteomics, Robert-Rössle-Strasse 10, D-13125 Berlin, Germany
[d] Institute of Biochemistry and Biotechnology, Martin Luther University Halle-Wittenberg, Kurt-Mothes-Strasse 3, D-06120 Halle (Saale), Germany

ARTICLE INFO

Article history:
Received 26 March 2013
Available online 10 April 2013

Keywords:
Autophosphorylation
Crystal structure
Hexokinase
Kluyveromyces lactis
KlHxk1
Phosphorylation

ABSTRACT

The bifunctional hexokinase KlHxk1 is a key component of glucose-dependent signal transduction in *Kluyveromyces lactis*. KlHxk1 is phosphorylated *in vivo* and undergoes ATP-dependent autophosphorylation-inactivation *in vitro*. This study identifies serine-15 as the site of *in vivo* phosphorylation and serine-157 as the autophosphorylation-inactivation site. X-ray crystallography of the *in vivo* phosphorylated enzyme indicates the existence of a ring-shaped symmetrical homodimer carrying two phosphoserine-15 residues. In contrast, small-angle X-ray scattering and equilibrium sedimentation analyses reveal the existence of monomeric phosphoserine-15 KlHxk1 in solution. While phosphorylation at serine-15 and concomitant homodimer dissociation are likely to be involved in glucose signalling, mechanism and putative physiological significance of KlHxk1 inactivation by autophosphorylation at serine-157 remain to be established.

1. Introduction

The enzyme subclass of hexokinases encloses bifunctional enzymes which, in addition to their catalytic function in glycolysis, are key components of glucose-dependent signal transduction [1–3]. Hexokinase involvement in glucose signalling is best understood in the Crabtree-positive yeast *Saccharomyces cerevisiae* where glucose abundance causes hexokinase isoenzyme ScHxk2 to translocate to the nucleus by interaction with the ScKap60 importin to form a complex including ScMig1 and ScSnf1 which prevents invertase expression [3]. By contrast, glucose limitation results in ScXpo1(ScCrm1)-dependent export of ScHxk2 into the cytosol. The nucleocytoplasmic translocation is stimulated *in vivo* by N-terminal phosphorylation of ScHxk2 at serine-15 decreasing the enzyme's affinity to ScKap60 and increasing its affinity to the ScXpo1 exportin [3]. *In vitro*, the same phosphorylation stimulates dissociation of the ScHxk2 homodimer [4], however, cellular functions of monomeric and dimeric phosphoserine-15 ScHxk2 are still a matter of debate. The phosphoenzyme is dephosphorylated in the cytosol by the ScGlc7-ScReg1 phosphoprotein phosphatase [5] to allow its nuclear import again when glucose is abundantly available. ScHxk2 is phosphorylated *in vitro* by autocatalysis at serine-158 in the presence of the glucose analogue D-xylose which is not phosphorylated by hexokinases. The autophosphorylation reaction is accompanied by a complete loss of glucose kinase activity which is fully reversed by enzymatic dephosphorylation of ScHxk2 [6], however, a physiological role of serine-158 phosphorylation remains to be established.

In contrast to the expression of two hexokinases (ScHxk1, ScHxk2), one glucokinase (ScGlk1) and one glucokinase paralog (ScEmi2) in *S. cerevisiae*, the genome of the Crabtree-negative yeast *Kluyveromyces lactis* in which no genome duplication has occurred [7] harbours a single hexokinase (KlHxk1). This enzyme is encoded by the *KlHXK1* (or *RAG5*) gene [8] and exhibits 73% identity with ScHxk2 [8]. *KlHXK1* mutants are affected in the expression of glucose transporters [8,9] and show relief from glucose repression of several enzymes [10,11]. The finding that glucose repression of invertase in *K. lactis* does not depend on KlMig1 [12] suggests the existence of different molecular mechanisms of glucose

Abbreviations: hrCNE, high-resolution clear native electrophoresis; SAXS, small-angle X-ray scattering.

* Corresponding author. Fax: +49 351 458 6305.
E-mail address: karina.kettner@tu-dresden.de (K. Kettner).

[1] These authors contributed equally to this work.
[2] Shares senior authorship.
[3] Present status: guest researcher at the Max Delbrück Center for Molecular Medicine (Berlin).

0006-291X/$ - see front matter © 2013 Elsevier Inc. All rights reserved.
http://dx.doi.org/10.1016/j.bbrc.2013.03.121

signalling in the two yeasts. Cross-complementation indicating the incompetence of KlHxk1 to restore glucose repression in *S. cerevisiae* is in support of this idea [8]. Recently, X-ray crystallography identified a symmetric ring-shaped dimer of N-terminally intact KlHxk1 [13] while crystals of ScHxk1 [14] and ScHxk2 [15] indicated monomers or non-symmetric dimers of inconclusive N-terminal integrity. The N-terminal stretch of 19 amino acids (V2-P20) of KlHxk1 that extends along the dimer interface [13] is highly similar to the N-terminus of ScHxk2 containing the *in vivo* phosphorylation site serine-15 [16]. This residue is progressively phosphorylated upon glucose exhaustion and is involved in the shuttle of ScHxk2 between cytosol and nucleus in *S. cerevisiae* [3]. In comparison, the functional role of the N-terminus of KlHxk1 is unknown but the detection of two molecular species of KlHxk1 exhibiting different isoelectric points (this paper) suggests the existence of a conserved phosphorylation site that is likely to correspond to serine-15 of ScHxk2. The observation that *in vitro* exposure of KlHxk1 to a condition causing complete autophosphorylation-inactivation of ScHxk2 [6] results in a partial inactivation of the *K. lactis* enzyme [11] might indicate another covalent modification, however, neither the site nor the mechanism and physiological significance are known.

The aim of the present work was to identify the presumed sites of *in vivo* phosphorylation and *in vitro* autophosphorylation-inactivation of KlHxk1 and to explore the structural consequences of *in vivo* phosphorylation as a basis of prospective functional studies. For this purpose, the *in vivo* phosphorylated KlHxk1 enzyme was isolated and crystallized and its structure analysed in the crystal and in solution. The experimental data support the view of KlHxk1 to play a key regulatory role in glucose-dependent signal transduction beyond its function as a glucose kinase.

2. Materials and methods

2.1. Strains and media

K. lactis strain JA6Δ*rag5R*/pTS*RAG5 (MATα, ade1–600 adeT-600 trp1–11 ura3–12, rag5::Scura3*) [11] was generated by transformation of JA6Δ*rag5R (rag5::Scura3*) with multicopy plasmid pTS*RAG5*. The latter strain was obtained from JA6Δ*rag5* (*rag5::ScURA3*; Wesolowski-Louvel, University of Lyon, France) by 5-fluoroorotic acid selection. JA6Δ*rag5* was constructed by *ScURA3* insertion into *RAG5* of wild type strain JA6 (*MATα, ade1–600 adeT-600 trp1–11 ura3–12* [17]). Cells were grown in YNB medium supplemented with amino acids [18] and 2% glucose at pH 5.5 and 30 °C.

2.2. Purification of unphosphorylated and in vivo phosphorylated KlHxk1

JA6Δ*rag5R*/pTS*RAG5* was grown overnight, re-cultivated in fresh medium for 90 min until an OD (600 nm/1 cm) of ~2, washed with yeast extract buffer (YEB, 50 mM potassium phosphate, pH 7.4, 1 mM EDTA) and stored at −80 °C. The frozen yeast was re-suspended in 3 ml YEB per gram wet cell pellet and subjected twice to French Pressure Cell Press (SLM Instruments) treatment at 138 MPa using the 40,000 psi standard cell. The supernatant obtained by protamine sulphate precipitation (0.2 mg/ml) and subsequent pH readjustment was chromatographed on a HiPrep 16/10 DEAE FF column (GE Healthcare) equilibrated with buffer A (20 mM Tris–HCl, pH 7.4). Proteins were eluted using a linear gradient from 0 to 1 M NaCl in buffer A. Fractions containing glucose-phosphorylating activity determined according to [19] were pooled and subjected to ammonium sulphate precipitation at 85% saturation. The precipitate was desalted, equilibrated with buffer A on PD-10 columns (GE Healthcare), applied onto a 6 ml Resource Q column (GE Healthcare) and fractionated using a linear gradient from 0 to 250 mM NaCl. Two protein species referred to as KlHxk1A and KlHxk1B subsequently eluting at increasing ionic strength and exhibiting glucose-phosphorylating activity were separated and precipitated with ammonium sulphate at 85% saturation. The precipitates were dissolved in buffer B (50 mM potassium phosphate containing ammonium sulphate at 50% saturation, pH 7.4) and subjected to hydrophobic interaction chromatography on a 1 ml Resource ETH column (GE Healthcare). Proteins were eluted by linearly decreasing the concentration of ammonium sulphate from 50 to 12.5% saturation, precipitated with ammonium sulphate at 85% saturation and stored at 4 °C. 1 mM DTT and 0.5 mM PMSF were present in all buffers.

2.3. In vitro autophosphorylation-inactivation of KlHxk1

The experimental conditions of autophosphorylation are described in [11]. Inactivation of purified KlHxk1A and KlHxk1B was monitored by measuring glucose kinase activity at different times using KlHxk1B incubated in the absence of ATP as a reference. Samples for mass spectrometry were taken after 24 h and precipitated with ammonium sulphate at 95% saturation.

2.4. Mass spectrometric identification of phosphorylation sites of KlHxk1

Mass determinations of unphosphorylated, *in vivo* phosphorylated and *in vitro* autophosphorylated KlHxk1 and analyses of their tryptic peptides were performed by ESI-MS and ESI-MS/MS on a Q-Tof Premier mass spectrometer (Waters Corporation) using the Mass Lynx 4.1 software (Waters Corporation). Experimental details and mass spectra are given in Supplementary data.

2.5. hrCNE analysis of KlHxk1 oligomerization

The hrCNE method was performed using cathode buffer variant 3 [20] and the HMW Native Marker Kit (GE Healthcare). The influence of phosphatase treatment was analysed by incubating KlHxk1A and KlHxk1B (2 μg each) with 200 U λ-phosphatase (New England Biolabs) for 1 h at 30 °C in the absence or presence of a mixture of phosphatase inhibitors (5 mM EDTA + Sigma–Aldrich phosphatase inhibitor cocktails 2 and 3) in a final volume of 20 μl.

2.6. Sedimentation equilibrium analysis of KlHxk1 oligomerization

KlHxk1A and KlHxk1B were analysed in an Optima™ XL-A analytical ultracentrifuge equipped with an An-50Ti rotor and 2-channel cells (Beckman Coulter) at loading protein concentrations of 0.70 mg/ml, respectively, in 50 mM potassium phosphate buffer, pH 7.4, containing 0.5 mM EDTA and 0.2 mM DTT. The enzymes were centrifuged at 10,000 rpm and 20 °C for 48 h with data collection at 280 nm. Weight average molecular weights were calculated by using the Optima™ XL-A/XL-I data analysis software (Beckman Coulter) applying a partial specific volume of 0.73 ml/g for both KlHxk1 species.

2.7. X-ray crystallography of in vivo phosphorylated KlHxk1

KlHxk1A (phosphorylated *in vivo* at serine-15 as demonstrated below) was equilibrated with crystallization buffer (10 mM Tris, 1 mM EDTA, 1 mM DTT, 0.5 mM PMSF, pH 7.4) on a Superdex 200 16/60 column (GE Healthcare). Peak fractions were pooled and concentrated using Vivascience 30 kDa molecular weight cut-off concentrating spin columns (VWR International) to adjust protein concentrations of 5–10 mg/ml. Crystallization was

accomplished at 291 K using hanging-drop 24-well plates filled with 0.5 ml crystallization solution and crystallization droplets composed of 1 µl KlHxk1 and 1 µl crystallization solution. Streak seeding was employed to improve reproducible crystal growth. Cuboid-shaped crystals of up to 250 µm length were obtained with crystallization solutions composed of 2.2 M ammonium phosphate and 0.1 M Tris–HCl at pH values of 8.0–8.5. Crystals were transferred in 1-min intervals to crystallization solutions supplemented with increasing amounts (2–5% per step) of glycerol to reach 20% (v/v) final concentration. X-ray data were collected at 100 K at beamline 14.2 of the BESSY synchrotron (Helmholtz Center Berlin) using a wavelength of 0.9141 Å. KlHxk1A crystallized in a crystal form of space group $P2_12_12_1$ (a = 105.8 Å, b = 178.3 Å, c = 216.2 Å). The analysed crystal diffracted to about 2.2 Å resolution. X-ray structure determination was performed as described in [13]. The asymmetric unit contained six chains (A-F) corresponding to three dimers (AD, BC, EF). For refinement, four TLS groups were defined per chain on the basis of an analysis by the TLS-MD server [21]. Structure quality indicators are listed in Supplementary data, Table S1.

2.8. SAXS analysis of in vivo phosphorylated KlHxk1

Measurements were conducted at the EMBL X33 beamline of the Deutsches Elektronen-Synchrotron (DESY Hamburg). KlHxk1A was equilibrated with crystallization buffer as described and diluted to obtain protein concentrations of 1, 3 and 6 mg/ml. Scattering patterns were recorded at 4 °C on a Pilatus 1 M-W pixel detector (Dectris, Baden, Switzerland) placed 2.7 m behind a 30 µl sample cell. This assembly covered a momentum transfer $s = 4\pi(\sin\theta)/\lambda$ of about 0.1–5 nm^{-1} at λ = 0.15 nm with 2θ representing the scattering angle. The processed and normalized scattering data collected during an exposure time of 300 s were corrected for buffer scattering and extrapolated to infinite dilution using PRIMUS [22]. The theoretical scattering intensities of the monomeric and dimeric models were calculated and fitted to the experimental data with CRYSOL [22] applying default settings. CRYSOL was also used for calculating the radii of gyration from the crystallographic models and from measured scattering data using automated constant subtraction. For *ab initio* envelope determination, the scattering data were processed by AutoGNOM [22]. DAMMIN [22] was subsequently used to calculate 10 independent modelling runs with no symmetry imposed. DAMSEL [22] was employed to generate the most probable model exhibiting the smallest discrepancy between all aligned model pairs. The models were averaged and further processed by DAMSUP, DAMAVER, and DAMFILT [22], respectively. Manual superimposing of shape envelope and protein coordinates was accomplished in PyMOL (www.pymol.org).

3. Results and discussion

3.1. Identity of the in vivo phosphorylation site of KlHxk1

Ion exchange chromatography of KlHxk1 extracted from glucose grown cells separated two molecular species tentatively referred to as KlHxk1A and KlHxkB (Fig. 1A). Hydrophobic interaction chromatography (Resource ETH, GE Healthcare) of both proteins and subsequent SDS–PAGE identified single protein bands of indistinguishable electrophoretic mobility corresponding to the molecular mass of the KlHxk1 subunit [11] (data not shown). ESI-MS measurements indicated a molecular mass of 53,558 ± 5 Da for KlHxk1A (Supplementary data, Fig. S1) which deviates by 79 Da from the value of 53,479 Da calculated for KlHxk1 lacking N-terminal methionine (http://www.uniprot.org/uniprot/P33284). By contrast, the analysis of KlHxk1B indicated a molecular mass of

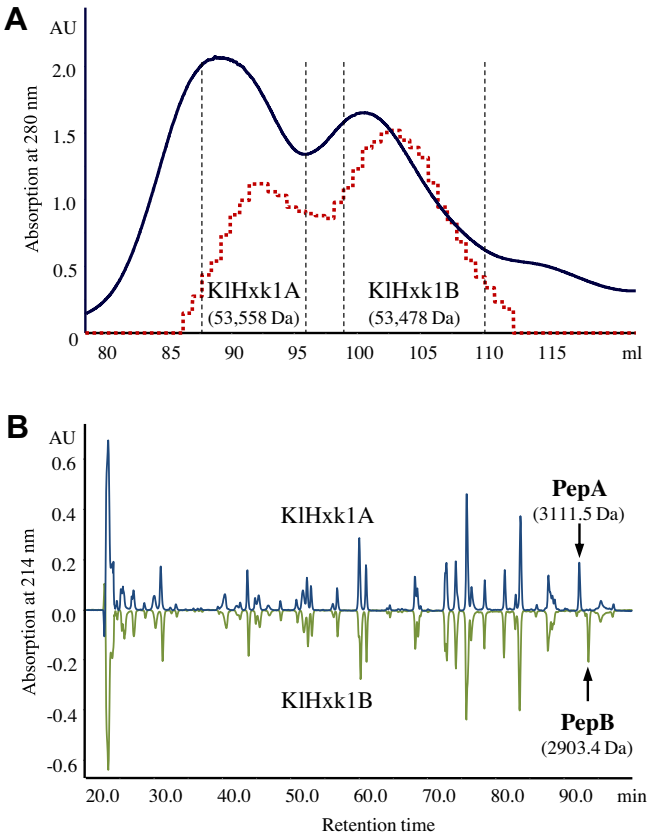

Fig. 1. Separation of unphosphorylated and serine-15 phosphorylated KlHxk1 and fractionation of corresponding tryptic peptides. (A) Resource Q chromatography of KlHxk1 pre-purified on HiPrep DEAE FF Sepharose 16/10. Solid line: absorbance at 280 nm; dotted line: glucose kinase activity. (B) µRPC C2/C18 SC 2.1/10 reverse phase separation of tryptic peptides generated from KlHxk1A and KlHxk1B finally purified by Resource ETH chromatography. Molecular masses determined by mass spectrometry are indicated in parentheses. KlHxk1A and PepA carry phosphoserine-15 while KlHxk1B and PepB are unphosphorylated.

53,478 ± 5 Da (Fig. S2) which is identical within the limits of experimental error with the value deposited in the UniProtKB database. In order to characterize the observed mass difference, tryptic digests of both KlHxk1 species were separated on a reverse-phase µRPC C2/C18 SC2.1/10 column (GE Healthcare) (Fig. 1B). ESI-MS analyses of peptides PepA and PepB each of which exclusively appearing in one of the two chromatograms revealed PepA to comprise amino acids K13-K40 and PepB to consist of amino acids G14-K40 (Figs. S3 and S4). Fragmentation of the PepA-derived most intense triple charged ion M^{3+} of m/z 1038.05 (Fig. S5) indicated phosphorylation at serine-15 (the only alternative being sulfation which was excluded by KlHxk1A dephosphorylation as outlined below) while fragmentation of the PepB-derived M^{3+} ion confirmed unphosphorylated serine-15 (Fig. S6). Taking into consideration both the structural similarity of the homologous hexokinases KlHxk1 and ScHxk2 and the influence of glucose availability on the phosphorylation of ScHxk2 at serine-15 [5,16], phosphorylation of KlHxk1 at the equivalent site may reflect a conserved mechanism of hexokinase modification contributing to glucose signalling in yeast. Presumably due to different growth conditions, phosphorylation of KlHxk1 at serine-15 has not been detected in previous studies [11].

3.2. Influence of serine-15 phosphorylation on KlHxk1 oligomerization

The impact of serine-15 phosphorylation on the monomer-homodimer equilibrium of KlHxk1 was analysed by hrCNE of

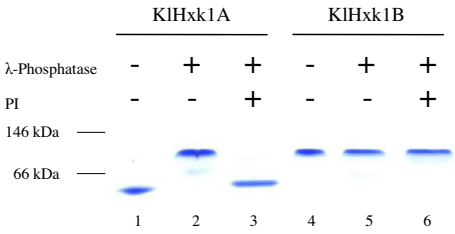

Fig. 2. hrCNE analysis of KlHxk1 oligomerization. KlHxk1A (lane 1) and KlHxk1B (lane 4) from Resource ETH chromatography were incubated for 1 h at 30 °C with λ-phosphatase in the absence (lanes 2 and 5) and presence (lanes 3 and 6) of phosphatase inhibitors (PI). Proteins were separated in 5–20% hrCNE gels and stained with Coomassie Blue R250. Molecular mass estimation is based on the migration of standard proteins covering the range from 66 to 669 kDa.

KlHxk1A and KlHxk1B representing serine-15-phosphorylated and unphosphorylated enzyme, respectively (Fig. 2). In case of KlHxk1A, the observed electrophoretic migration indicated an estimated molecular mass of ~50 kDa (lane 1) which corresponds to the KlHxk1 subunit [11]. By contrast, the estimated value of ~100 kDa of KlHxk1B (lane 4) refers to the homodimeric enzyme [11]. In accordance with these findings, the electrophoretic mobility of phosphatase-treated KlHxk1A (lane 2) was identical to that of the unphosphorylated enzyme (lane 4), and phosphatase inhibition maintained the monomeric state (lane 3), while neither phosphatase nor inhibitor treatment affected the electrophoretic migration of KlHxk1B (lanes 5 and 6). Taken together, the electrophoretic behaviour of the two KlHxk1 species confirms the existence of a phosphorylation site in KlHxk1A and suggests phosphorylation of KlHxk1B at serine-15 to promote the dissociation of the homodimeric enzyme.

3.3. Crystal structure of serine-15 phosphorylated KlHxk1

In the crystal, purified KlHxk1A forms a ring-shaped symmetrical homodimer (Fig. 3A) which has the same architecture as the previously crystallized unphosphorylated KlHxk1 [13]. The corresponding X-ray data and refinement statistics are given in Supplementary data, Table S1. Dimerization stabilizes the observed conformation of the N-terminus which likely is flexible when monomeric KlHxk1 is formed in solution. As a consequence, two phosphoserine-15 residues are visible in the electron density maps of the two intersubunit interfaces of the crystallized KlHxk1A homodimer (Fig. 3B). The identification of a homodimeric arrangement of phosphoserine-15 KlHxk1 does not contradict the results of hrCNE (Fig. 2) since dimerization is likely due to the extremely high concentration of the KlHxk1A protein in the crystal (540 mg/ml corresponding to 10.1 mM monomer) where the dimer is also stabilized by crystal packing interactions.

3.4. Crystal vs. solution structure of serine-15 phosphorylated KlHxk1

The electrophoretic analysis of KlHxk1 oligomerization indicated the formation of monomers as a consequence of serine-15 phosphorylation (Fig. 2). By contrast, homodimers of the same phosphoserine-15 enzyme were detected in the crystal (Fig. 3). In order to verify the existence of monomeric phosphoserine-15 KlHxk1 in solution, the two KlHxk1 species were subjected to sedimentation equilibrium analysis. Taking into account the dissociation constant K_D = 0.15 μM of the unphosphorylated enzyme [11], KlHxk1B was expected to predominantly exist in the dimeric state at the loading enzyme concentration corresponding to 14 μM KlHxk1 monomer. Indeed, the radial distribution of KlHxk1B at sedimentation equilibrium (Fig. 4A, open circles) corresponds to a calculated weight average molecular weight of 98 kDa and fits well to the theoretical molecular mass of 107 kDa of the homodimer [11]. In comparison, the equilibrium distribution of KlHxk1A (Fig. 4A, full circles) corresponds to a calculated weight average molecular weight of 52 kDa confirming serine-15 phosphorylation to cause monomer formation in solution. The latter conclusion is supported by the outcome of a SAXS analysis of KlHxk1 oligomerization (Fig. 4B and C). The experimentally determined radius of gyration of 25.7 ± 0.1 Å of KlHxk1A is almost identical with the value of 26.1 ± 0.5 Å calculated for the KlHxk1A monomers present in the crystals, but deviates significantly from the value of 31.2 Å ± 0.1Å calculated for the crystallized KlHxk1A homodimers. In addition, substantial coincidence of the scattering curve calculated for the KlHxk1A monomer and the experimental scattering data of

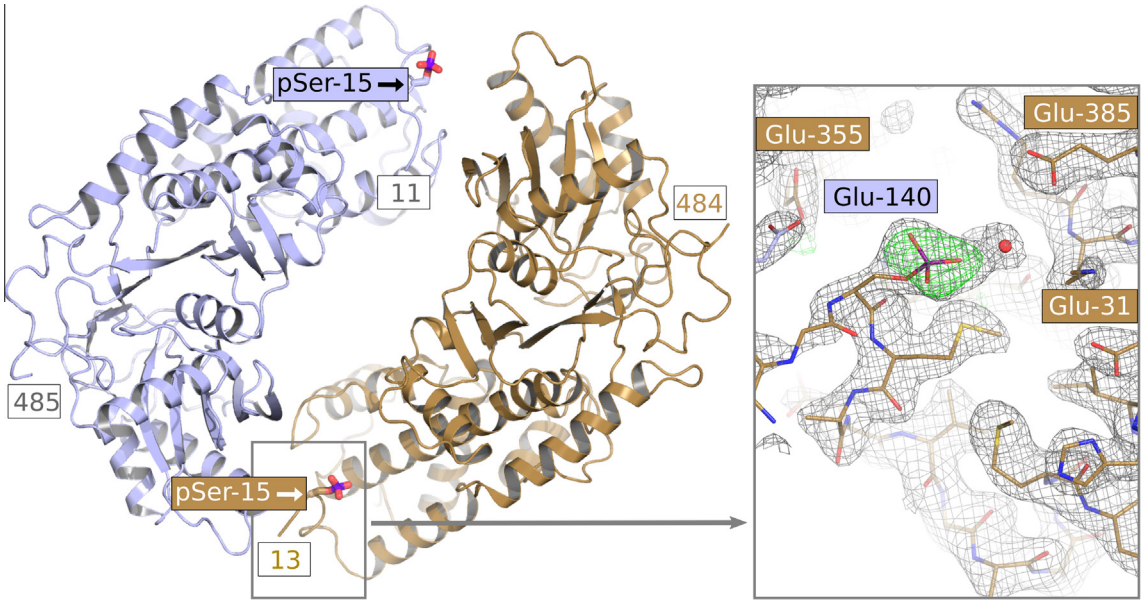

Fig. 3. X-ray structure of serine-15 phosphorylated KlHxk1. (A) Ring-shaped homodimer of KlHxk1A (BC dimer of the asymmetric unit). Phosphoserine-15 residues are shown as stick models (blue: phosphorus; red: oxygen). Numbers define terminal residues. (B) Electron density maps (grey: $2F_o - F_c$ at 1σ contour level; green: omit $F_o - F_c$ at 3σ contour level) of phosphoserine-15 (chain B) and its environment. The red sphere represents a water molecule.

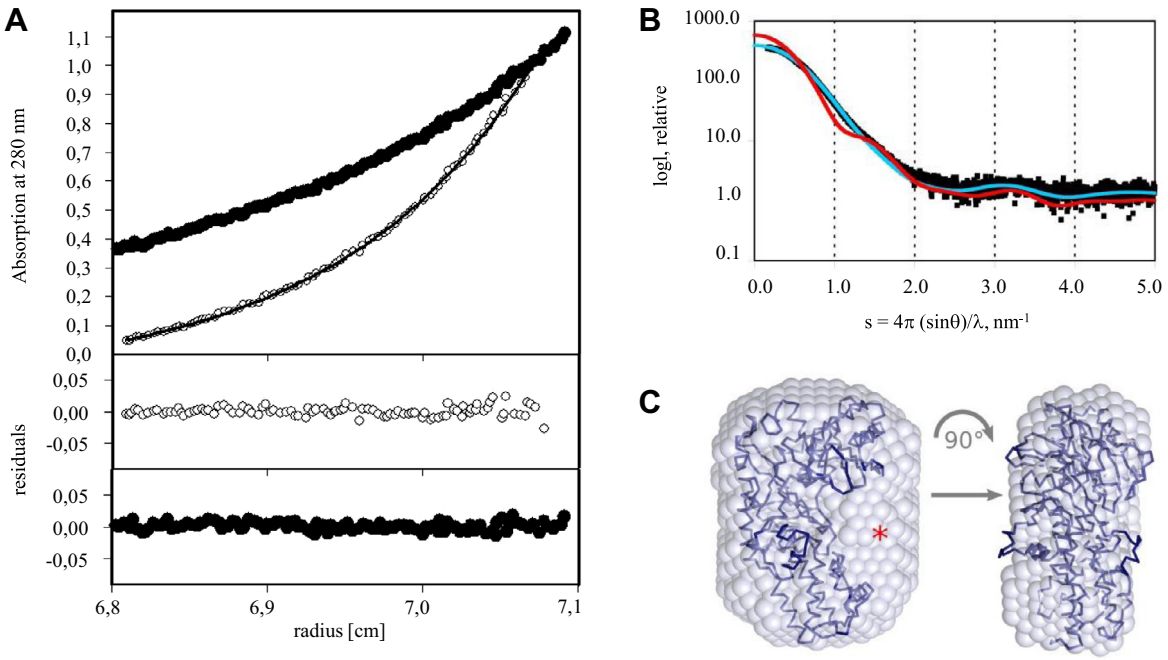

Fig. 4. Sedimentation equilibrium and SAXS analysis of KlHxk1 oligomerization. (A) Weight average molecular weights of KlHxk1A (phosphorylated at serine-15; ●) and KlHxk1B (unphosphorylated; ○) were determined by equilibrium sedimentation performed at 10,000 rpm and 20 °C. Loading enzyme concentrations were 0.70 mg/ml, respectively. Protein distributions (solid lines) were fitted to single molecular species of M_r = 52,000 for KlHxk1A and M_r = 98,000 for KlHxk1B. Lower panels: deviations of fit and experimental data. (B) SAXS data of KlHxk1A analysed at protein concentrations of 1, 3 and 6 mg/ml (black squares; merged data). The calculated scattering curves for monomeric KlHxk1A (amino acids 15–485 of chain E of the asymmetric unit) and dimeric KlHxk1A (Fig. 3A, BC dimer) are printed in blue and red, respectively. (C) SAXS *ab initio* shape model of KlHxk1A in solution (light blue spheres) with manually positioned crystallographic model (blue). Asterisk: Putative location of missing N-terminus (amino acids 2–14) of the crystallographic model.

the serine-15 phosphorylated enzyme was observed (Fig. 4B) with a discrepancy value of χ^2 = 1.17. By contrast, the scattering curve calculated for the KlHxk1A homodimer exhibits a poor fit (χ^2 = 6.46). Based on the SAXS data, an envelope model of KlHxk1 was computed by *ab initio* shape reconstruction (Fig. 4C). The resulting model accommodates the KlHxk1A monomer but not the homodimer. Minor differences between envelope shape and crystallographic model are probably due to the missing N-terminus in the crystallographic model, the larger flexibility of the enzyme in solution and/or the lower resolution of SAXS which precludes a more precise shape determination. The formation of monomers of KlHxk1A in solution may be explained by electrostatic repulsions of the two negatively charged phosphoserine-15 groups with nearby negatively charged residues (Glu-31, Glu-355 and Glu-385) of the adjacent subunit (Fig. 3B) and by the significantly lower concentration of the enzyme in solution compared to the situation in the crystal [13].

The comparison of crystal and solution structures of phosphoserine-15 KlHxk1 supports the view that phosphorylation at serine-15 allows monomer formation at enzyme concentrations that according to the law of mass action would impede dissociation of the unphosphorylated homodimeric enzyme otherwise. Recently, protein kinases Tda1/Ymr291w [23] and Snf1 [3] were reported to be implicated in the phosphorylation of the homologous hexokinase ScHxk2 at serine-15 in response to glucose limitation [5,16], but neither the condition triggering KlHxk1 phosphorylation at the equivalent site nor the corresponding kinase is known. Taking into consideration the existence of a gene in *K. lactis* encoding a hypothetical protein which is homologous to the Tda1/Ymr291w protein kinase (http://www.uniprot.org/uniprot/Q6CXB5), similar functional roles for KlHxk1 and the upstream KlHxk1 serine-15 kinase in glucose dependent signal transduction in *K. lactis* seem conceivable.

3.5. Identity of the autophosphorylation-inactivation site of KlHxk1

The site modified *in vitro* by ATP-dependent autophosphorylation [11] was determined by monitoring the kinetics of inactivation of KlHxk1A and KlHxk1B followed by mass spectrometry. Fragmentation analysis of tryptic peptides identified serine-157 as the sole site of autophosphorylation of both KlHxk1 species (Supplementary data, Figs. S7–S10). In contrast to ScHxk2 where inactivation by autophosphorylation was complete within minutes [6], both KlHxk1A and KlHxk1B retained a residual catalytic activity of ~30% even after long-term exposure (30 h) to autophosphorylation conditions (data not shown). The kinetics of autophosphorylation-inactivation are not appropriate, however, to discriminate between a reduced molecular catalytic activity as a consequence of serine-157 phosphorylation and the existence of a mixture of non-autophosphorylated and autophosphorylated enzyme species the former being catalytically fully active and the latter being less active or inactive. Physiological conditions promoting autophosphorylation-inactivation of KlHxk1 in *K. lactis* have not been identified so far. The effective inhibition of glucose kinase activity, however, provokes the idea of KlHxk1 autophosphorylation at serine-157 to represent a molecular switch determining the rate of glycolysis while phosphorylation *in vivo* at serine-15 might be implicated in the transcriptional control of glucose metabolism as suggested for the homologous hexokinase ScHxk2 of *S. cerevisiae*[3]. The outcome of a proteomic analysis of KlHxk1 deficiency in *K. lactis* indicating a key regulatory role of the enzyme in central metabolism and beyond (N. Mates and K. Kettner, unpublished) is in line with the latter conclusion. Functional studies of KlHxk1 mutants constructed by site-directed mutagenesis at amino acid positions 15 and/or 157 are expected to disclose the regulatory significance of KlHxk1 phosphorylation at either site.

Acknowledgements

We thank the Helmholtz-Zentrum Berlin (Germany) and the EMBL Hamburg Outstation at DESY (Germany) for synchrotron beam time and travel support, Susanne Moschütz and Antje Keim for technical support, Clemens Scholtysik for model building and the Bioanalytics group of the Center for Biotechnology and Biomedicine at Leipzig University for mass spectroscopy.

Appendix A. Supplementary data

Supplementary data associated with this article can be found, in the online version, at http://dx.doi.org/10.1016/j.bbrc.2013.03.121.

References

[1] F.M. Matschinsky, M.A. Magnuson, D. Zelent, T.L. Jetton, N. Doliba, Y. Han, R. Taub, J. Grimsby, The network of glucokinase-expressing cells in glucose homeostasis and the potential of glucokinase activators for diabetes therapy, Diabetes 55 (2006) 1–12.

[2] F. Rolland, E. Baena-Gonzalez, J. Sheen, Sugar sensing and signaling in plants: conserved and novel mechanisms, Annu. Rev. Plant Biol. 57 (2006) 675–709.

[3] P. Fernandez-Garcia, R. Pelaez, P. Herrero, F. Moreno, Phosphorylation of yeast hexokinase 2 regulates its nucleocytoplasmic shuttling, J. Biol. Chem. 287 (2012) 42151–42164.

[4] J. Behlke, K. Heidrich, M. Naumann, E.C. Müller, A. Otto, R. Reuter, T. Kriegel, Hexokinase 2 from *Saccharomyces cerevisiae*: regulation of oligomeric structure by *in vivo* phosphorylation at serine-14, Biochemistry 37 (1998) 11989–11995.

[5] F. Randez-Gil, P. Sanz, K.D. Entian, J.A. Prieto, Carbon source-dependent phosphorylation of hexokinase PII and its role in the glucose-signaling response in yeast, Mol. Cell Biol. 18 (1998) 2940–2948.

[6] K. Heidrich, A. Otto, J. Behlke, J. Rush, K.W. Wenzel, T. Kriegel, Autophosphorylation-inactivation site of hexokinase 2 in *Saccharomyces cerevisiae*, Biochemistry 36 (1997) 1960–1964.

[7] C. Seoighe, K.H. Wolfe, Yeast genome evolution in the post-genome era, Curr. Opin. Microbiol. 2 (1999) 548–554.

[8] C. Prior, P. Mamessier, H. Fukuhara, X.J. Chen, M. Wesolowski-Louvel, The hexokinase gene is required for transcriptional regulation of the glucose transporter gene *RAG1* in *Kluyveromyces lactis*, Mol. Cell Biol. 13 (1993) 3882–3889.

[9] P. Billard, S. Menart, J. Blaisonneau, M. Bolotin-Fukuhara, H. Fukuhara, M. Wesolowski-Louvel, Glucose uptake in *Kluyveromyces lactis*: role of the *HGT1* gene in glucose transport, J. Bacteriol. 178 (1996) 5860–5866.

[10] P. Goffrini, A. Ficarelli, I. Ferrero, Hexokinase activity is affected in mutants of *Kluyveromyces lactis* resistant to glucose repression, Microbiology 141 (1995) 441–447.

[11] D. Bär, R. Golbik, G. Hübner, H. Lilie, E.C. Müller, M. Naumann, A. Otto, R. Reuter, K.D. Breunig, T.M. Kriegel, The unique hexokinase of *Kluyveromyces lactis*. Molecular and functional characterization and evaluation of a role in glucose signaling, J. Biol. Chem. 278 (2003) 39280–39286.

[12] I. Georis, J.P. Cassart, K.D. Breunig, J. Vandenhaute, Glucose repression of the *Kluyveromyces lactis* invertase gene *KlINV1* does not require Mig1p, Mol. Gen. Genet. 261 (1999) 862–870.

[13] E.B. Kuettner, K. Kettner, A. Keim, D.I. Svergun, D. Volke, D. Singer, R. Hoffmann, E.C. Müller, A. Otto, T.M. Kriegel, N. Sträter, Crystal structure of hexokinase KlHxk1 of *Kluyveromyces lactis*: a molecular basis for understanding the control of yeast hexokinase functions *via* covalent modification and oligomerization, J. Biol. Chem. 285 (2010) 41019–41033.

[14] P. Kuser, F. Cupri, L. Bleicher, I. Polikarpov, Crystal structure of yeast hexokinase PI in complex with glucose: A classical "induced fit" example revised, Proteins 72 (2008) 731–740.

[15] P.R. Kuser, S. Krauchenco, O.A. Antunes, I. Polikarpov, The high resolution crystal structure of yeast hexokinase PII with the correct primary sequence provides new insights into its mechanism of action, J. Biol. Chem. 275 (2000) 20814–20821.

[16] T.M. Kriegel, J. Rush, A.B. Vojtek, D. Clifton, D.G. Fraenkel, *In vivo* phosphorylation site of hexokinase 2 in *Saccharomyces cerevisiae*, Biochemistry 33 (1994) 148–152.

[17] K.D. Breunig, P. Kuger, Functional homology between the yeast regulatory proteins GAL4 and LAC9: LAC9-mediated transcriptional activation in *Kluyveromyces lactis* involves protein binding to a regulatory sequence homologous to the GAL4 protein-binding site, Mol. Cell Biol. 7 (1987) 4400–4406.

[18] F. Sherman, G.R. Fink, J.B. Hicks, Laboratory Course Manual for Methods in Yeast Genetics, Cold Spring Harbor Laboratory Press, Cold Spring Harbor, NY, 1986.

[19] K. Kettner, E.C. Müller, A. Otto, G. Rödel, K.D. Breunig, T.M. Kriegel, Identification and characterization of a novel glucose-phosphorylating enzyme in *Kluyveromyces lactis*, FEMS Yeast Res. 7 (2007) 683–692.

[20] I. Wittig, M. Karas, H. Schägger, High resolution clear native electrophoresis for in-gel functional assays and fluorescence studies of membrane protein complexes, Mol. Cell Proteomics 6 (2007) 1215–1225.

[21] J. Painter, E.A. Merritt, Optimal description of a protein structure in terms of multiple groups undergoing TLS motion, Acta Crystallogr. D Biol. Crystallogr. 62 (2006) 439–450.

[22] M.V. Petoukhov, D. Franke, A.V. Shkumatov, G. Tria, A.G. Kikhney, M. Gajda, C. Gorba, H.D.T. Mertens, P.V. Konarev, D.I. Svergun, New developments in the ATSAS program package for small-angle scattering data analysis, J. Appl. Cryst. 45 (2012) 342–350.

[23] K. Kettner, U. Krause, S. Mosler, C. Bodenstein, T.M. Kriegel, G. Rödel, *Saccharomyces cerevisiae* gene *YMR291W/TDA1* mediates the *in vivo* phosphorylation of hexokinase isoenzyme 2 at serine-15, FEBS Lett. 586 (2012) 455–458.